Progress In Electromagnetics Research C, Vol. 133, 51–63, 2023

A Novel Wideband Beamforming Antenna for 5G Applications by Eliminating the Phase Shifters and Crossovers from the Butler Matrix

Aicha Bembarka[1, *], Larbi Setti[1], Abdelwahed Tribak[2], Hafid Tizyi[2], and Mohssine El Ouahabi[3]

Abstract—In this study, a novel Switched Beam Antenna (SBA) system is proposed and experimentally validated for C-band applications. The system is made up of a 4×4 Butler matrix, whose outputs are connected to four square-looped radiator antenna elements. The originality of the proposed work depends on the construction of a miniaturized beamforming network with minimal complexity, low loss, and low expense. Moreover, designing a system with a broad frequency range enables its use in a variety of applications. Miniaturization is achieved by eliminating the crossover and integrating the 45° shifter into the 90° hybrid coupler, as well as tilting the antenna array (i.e., making the Butler matrix output and the feed line of the antenna element orthogonal). The simulated results of the phase difference between the suggested Butler matrix outputs closely match the −45°–135° theoretical calculations. The SBA measured results show a wide bandwidth and low insertion loss of 63.64% (4.21–8.14 GHz) and −4.89 dB, respectively. Four orthogonal beams are produced by the proposed structure's input ports 1–4 when they are excited. These beams are aligned at angles of −10°, 60°, −60°, and 10° at 5.7 GHz.

1. INTRODUCTION

It is noteworthy nowadays that there is a bulky demand for smart devices with wireless communications, which is accompanied by enormous channel congestion, resulting in signal interference. Furthermore, during wireless transmission, the transmitted signal strength may be attenuated and faded [1, 2]. An effective method for reducing multipath fading and improving the performance of wireless networks is antenna diversity [3]. According to research, frequency diversity antennas helped lower signal correlation and prevent any potential connection issues, like in [4]. The switching ability in radiation pattern diversity can greatly enhance the connection margin while suppressing co-channel interference by directing the energy precisely toward the required direction [5]. Switched beamforming antenna array technology is a type of antenna array system that uses a simpler and less complex algorithm than other beamforming techniques, such as digital beamforming.

For the sake of forming a flexibly changed beam angle, the beamforming steering networks are typically required to adapt the phase of the individual signals in the antenna array, which may be accomplished by utilizing what is known as feeding matrices. The Butler matrix [6], Blass matrix [7], and Nolen matrix [8] are the most well-known versions in which couplers are the fundamental components in the construction of these matrices. Unfortunately, the Blass and Nolen matrices are more complicated

Received 7 February 2023, Accepted 15 May 2023, Scheduled 23 May 2023
* Corresponding author: Aicha Bembarka (aichabembarka@gmail.com).
[1] Laboratory of Sciences and Advanced Technologies (LSTA), Polydisciplinary Faculty of Larache (FPL), Abdelmalek Essaadi University, Tetouan, Morocco. [2] Department of Electronics Microwaves and Optics, National Institute of Posts and Telecommunications (INPT), Rabat, Morocco. [3] Department of Civil and Industrial Sciences and Technologies, National School of Applied Sciences (ENSA), Abdelmalek Essaadi University, Tetouan, Morocco.

and need more couplers than the Butler matrix, and they require doubling the number of terminating resistive loads. As a result, the Butler matrix has become the mainstream technique for switching beam systems [9].

Most of the switched beam systems that rely on the Butler matrix are designed using conventional crossovers and phase shifters or other components [10–13]. The 4×4 Butler matrices in [10, 12, 13] are made up of four hybrid couplers, two crossovers, and two 45° phase shifters, and they are developed using the multilayer substrate technology. An exception is made in [14] where the complementary split ring resonators loaded transmission lines were used instead of phase shifters. All of these antennas failed to account for the space that may be used to cover the antenna. Following that, several publications emphasize simplicity and size reduction while maintaining high performance. Some researchers removed the 45° phase shifter from the conventional Butler matrix to reduce the size and avoid connectivity mismatch loss and unbalanced amplitude. The 45° phase shifter was eliminated and instead incorporated into the quadrature hybrid coupler in [14] or into the crossover in [15]. Because crossover manufacturing is a bit complicated, more accuracy is required to minimize loss, which results in increased expenses. The authors of [16] merely removed the crossover and then provided open stubs for the branch line coupler transmission lines to further miniaturize the Butler matrix, yielding a Butler matrix with dimensions of $2.01\lambda_g \times 1.13\lambda_g$ at 2.5 GHz. Another crossover elimination was carried out in [17] providing an 8×8 and a 4×4 Butler matrices operating at 1.9 GHz and 2.44 GHz, respectively.

For further simplification, the simultaneous removal of the phase shifter and crossover has been mentioned in certain papers, such as in [18] and [19]. Aside from miniaturization, multi-functionality in current wireless systems for cost reduction is another key strategy, which may be attained by increasing antenna impedance bandwidth. References [18] and [19] were solely concerned with miniaturization and ignored the bandwidth coverage, which is barely 10% and 17.28%, respectively. On the other hand, as shown in [20], various designs of wideband beamforming antennas have been published in the literature. [20] presented two topologies with ultra-wideband bandwidths ranging from 3.1 to 10.6 GHz without the use of crossover. The first topology uses a lozenge-shaped Butler matrix conductor, whereas the second uses elliptical-shaped conductors. Unfortunately, their limitations include their extremely large size as a result of the multilayer technology utilized, which increases the difficulty of manufacturing.

In contrast to the studies previously mentioned, which all concentrated on either miniaturization or multi-functionality, we merged the two in our antenna. The proposed structure was reduced in size by deleting the crossover and phase shifters, as well as employing a tilted antenna array rather than a normal positioning antenna array. For the Butler matrix bandwidth improvement, the well-known technique of integrating crossed transmission lines into the traditional coupler as in [21, 22] has been employed. Therefore, a new SBA that covers a wide fractional bandwidth of almost 63.64%, resonating in the C-Band between 4.21 and 8.14 GHz, is proposed in this paper. The switching mechanism among four beams directed toward four different angles −10°, 60°, −60°, and 10° at 5.7 GHz is simply adjusted by exciting one port from the four input ports and terminating the others by an impedance of 50Ω. This antenna has an overall size of $70.36 \times 59.41 \times 0.81\,\text{mm}^3$. Manufacturing has been successfully done for the proposed structure. This article is divided into several sections: a theoretical study of the proposed feeding network is presented in Section 2, and its results are covered in Section 3. Section 4 discusses the suggested SBA results (S-parameters, radiation pattern, gain and radiation efficiency), followed by a conclusion in Section 5.

2. THEORETICAL STUDY

In general, designing a Butler matrix needs the use of phase shifters and directional couplers. In consequence, a 4×4 Butler matrix requires four directional couplers (3 dB, 90°), two 45° phase shifters, and two crossovers, as seen in Fig. 1 [23]. By stimulating the input ports of the matrix, numbered from 1 to 4, four output signals that have equal power but with distinct phases are produced, numbered from 5 to 8. The traditional Butler matrix depicted in Fig. 2(a) has been simplified to achieve the suggested Butler matrix topology illustrated in Fig. 2(b). Big letters numbered from A to H are added to the conventional matrix to make signal tracking easier.

The Butler matrix contains several output beams, hence the beam's phase difference needs to be consistent to prevent interference between the beams. To put it another way, in terms of scattering

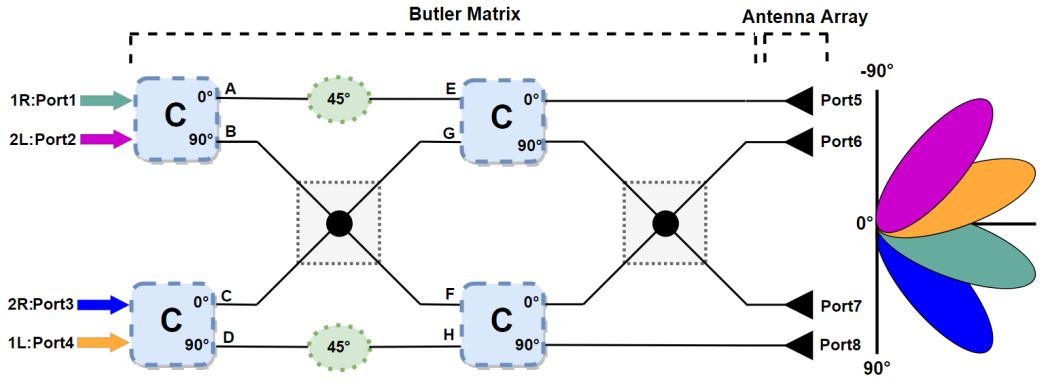

Figure 1. Beamforming antenna array block diagram.

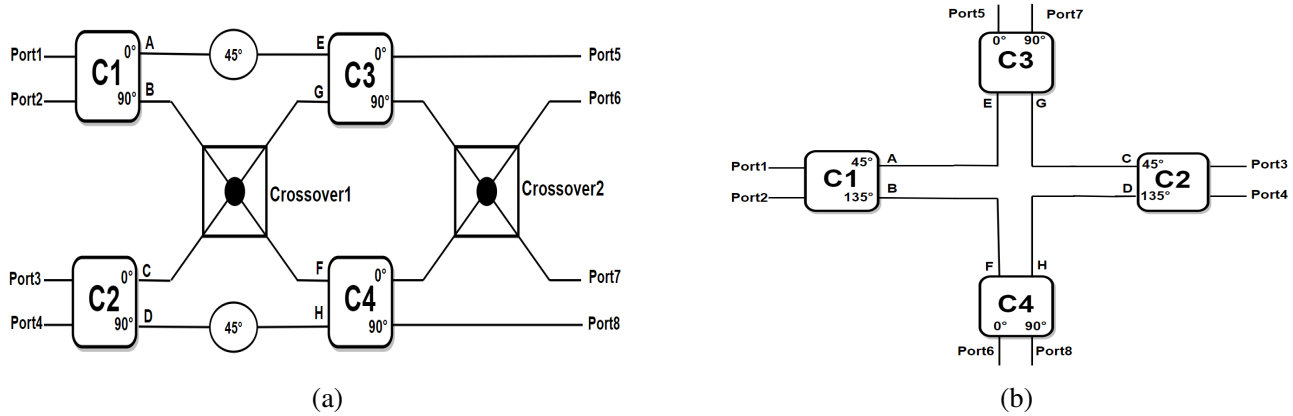

(a) (b)

Figure 2. 4×4 Butler matrix schematic. (a) Traditional and (b) suggested.

parameters, the phase difference must meet the equality of the three equations in (1):

$$\angle S(6,X) - \angle S(5,X) = \angle S(7,X) - \angle S(6,X) = \angle S(8,X) - \angle S(7,X) \tag{1}$$

where X refers to the exciting port; 1, 2, 3, or 4.

Denote the resulting phases at port 5 and port 6 by α and ϕ, respectively. With port 1 fed, the phase at port 7 is $\alpha + \phi$, and its value at port 8 is equal to $\phi + \phi$. In the traditional Butler matrix of Fig. 2(a), α is achieved by following the route 'AE' which concerns two 0° phase lags from the direct path of the 90° directional couplers and 45° lag from the phase shifter, then port 5 gets the phase α equal to $-45°$ or 45°. When α is $-45°$, ϕ has $-90°$ because of following the 'BF' path. This phase value is achieved by passing the port 1 signal to the coupled port of the first coupler, then going through the first 0 dB crossover getting to port 6 via the direct path of the fourth coupler and second crossover. In order to get the phase at ports 7 and 8 the signals will follow the paths 'AE' and 'BF', but this time the coupler ports of the third and fourth couplers will be used in the paths, respectively. Therefore, at port 7 the output phase is equal to $-135°$ whereas at port 8 it is $-180°$. The same phase difference for the successive ports is given by Equation (2) for port 1 [16]. Therefore,

$$\begin{aligned} \angle S(6,1) - \angle S(5,1) &= -90 - (-45) = -45° \\ \angle S(7,1) - \angle S(6,1) &= -135 - (-90) = -45° \\ \angle S(8,1) - \angle S(7,1) &= -180 - (-135) = -45° \end{aligned} \tag{2}$$

If we apply the same procedure in the excitation of port 2, and the phase at port 5 is -45, we will receive a phase difference of 135° between the sequenced ports. Ports 3 and 4 are the symmetry of ports 2 and 1. As a result, when port 3 is fed, the Butler matrix yields a $-135°$ phase between the sequenced ports, and in the case of port 4 feed, it is 45°.

The crossover also referred to as 0 dB coupler is a four terminals component composed of two hybrid couplers cascaded together. Its primary feature is that all power entered must reach the output port existing on the other side of the transmission line. In the conventional crossover, the signal must pass over three quarter-wavelength transmission lines, requiring a high electrical size and increasing the chance of signal loss, which might adversely impact the system's performance. Because the losses decrease as the number of lines decreases, eliminating the 0 dB coupler and integrating the 45° phase shifter into the 90° coupler is the best choice. The phase difference for the simplified Butler matrix is determined as shown in Equation (3) by port 1 excited, as an example: the signal travels via the route '1A-AE-E5' to port 5 with a 135°. When the signal follows the '1B-BF-F6' path, port 1 and port 6 experience a 90° phase shift. The signal also travels over the '1A-AE-E7' route, which between ports 1 and 7 results in a 45° phase shift. When the signal follows the path '1B-BF-F8' there is a 0° of phase shift between ports 1 and 8.

$$\begin{aligned}
\angle S(5,1) &= \angle(1,A) + \angle(A,E) + \angle(E,5) = 135^\circ + 0^\circ + 0^\circ = 135^\circ \\
\angle S(6,1) &= \angle(1,B) + \angle(B,F) + \angle(F,6) = 90^\circ + 0^\circ + 0^\circ = 90^\circ \\
\angle S(7,1) &= \angle(1,A) + \angle(A,E) + \angle(E,7) = 135^\circ + 0^\circ - 90^\circ = 45^\circ \\
\angle S(8,1) &= \angle(1,B) + \angle(B,F) + \angle(F,8) = 90^\circ + 0^\circ - 90^\circ = 0^\circ
\end{aligned} \tag{3}$$

As in Equation (2), we get a phase difference equal to -45° between the successive ports for port 1. Similar calculations may be conducted for the phase shifts between input and output ports if the signal is generated on the other input ports. Therefore, the simplified Butler matrix in Fig. 2(b) provides the same phase difference between the sequenced output ports as the conventional Butler matrix. The excitation of ports 1, 2, 3, and 4 results accordingly in output phase differences of -45°, 135°, -135°, and 45°. The results of our Butler matrix are presented in Subsection 3.2, which proves the theoretical calculations.

3. PROPOSED WIDEBAND 4 × 4 BUTLER MATRIX

Designing an SBA that covers a wide frequency range necessitates the construction of a wideband Butler matrix, which in turn requires the use of wideband couplers. To enhance the bandwidth of the couplers, we connected the four lines of the conventional coupler with orthogonal crossed lines at their center (two-crossed transmission lines). The two-crossed lines introduce additional degrees of freedom, allowing for more design flexibility, optimization, and better performance.

3.1. Couplers Design

As previously indicated, the suggested Butler matrix has two 90° and two 45° (135°/45°) couplers. For that purpose, these couplers are designed and optimized separately first. After that, they are gathered together following the schematic in Fig. 2(b). These couplers have a broad bandwidth as proven below. We used Equations (4) and (5) of [24] to calculate the impedance Z_c of the lines of the couplers, and all designs are constructed on a single-layered Rogers substrate that has relative permittivity $\epsilon_r = 3.38$ and high $h = 0.813$ mm.

$$A = \frac{Z_c}{60} * \sqrt{\frac{\epsilon_r + 1}{2}} + \frac{\epsilon_r - 1}{\epsilon_r + 1}\left(0.23 + \frac{0.11}{\epsilon_r}\right) \tag{4}$$

$$W = \frac{8he^A}{e^{2A} - 2} \tag{5}$$

The 90° hybrid coupler scattering parameters and phase between its output ports 3 and 4 simulated results are presented in Fig. 3. They have been taken with port 1 excited. It can be clearly noticed from the graph in Fig. 3(b) that this first designed coupler has almost -88.564° phase difference between its outputs with only $\pm 3.5^\circ$ phase variation. As seen from Fig. 3(a), the coupler 10-dB return loss resonance is between 4.47 and 8.62 GHz, which is interpreted by 63.4% of fractional bandwidth. Besides, it has an isolation $S(2,1)$ of -22.7 dB at 6 GHz. The 90° hybrid coupler is known for its limited bandwidth [25], and for that purpose, we added two-crossed transmission lines at the center of the coupler to expand its

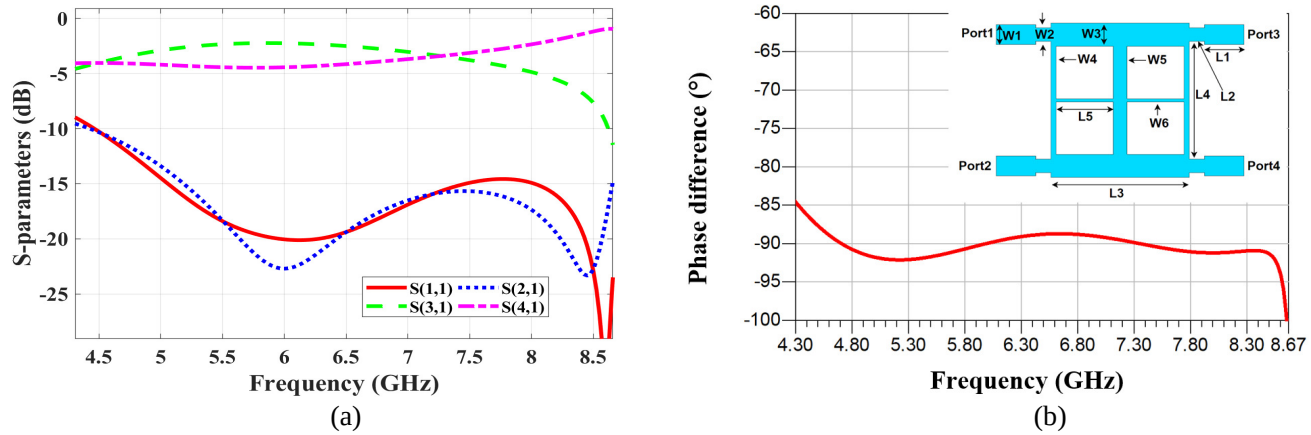

Figure 3. (a) S-parameters and (b) phase difference simulated results of the suggested 90° coupler ($W1 = 1.9$, $W2 = 1.3$, $W3 = 2.2$, $W4 = 0.5$, $W5 = 1.3$, $W6 = 0.3$, $L1 = 3.71$, $L2 = 1.41$, $L3 = 13$, $L4 = 11.20$, $L5 = 5.35$ in mm unit).

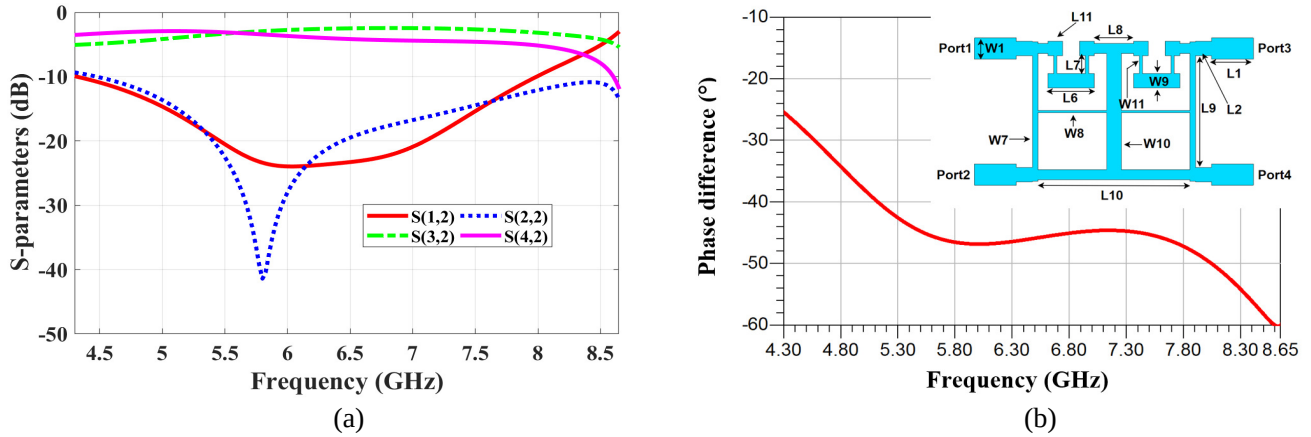

Figure 4. (a) S-parameters and (b) phase difference simulated results of the suggested 135°/45° coupler. ($W1 = 1.9$, $W2 = 1.3$, $W7 = 0.5$, $W8 = 0.2$, $W9 = 1.3$, $W10 = 1.3$, $W11 = 0.3$, $L1 = 3.71$, $L6 = 4.1$, $L7 = 1.6$, $L8 = 3.46$, $L9 = 10.07$, $L10 = 13.4$, $L11 = 1.3$ in mm unit).

bandwidth. Optimized parameters of the coupler are presented in Fig. 3 which are in millimeter units. As noticed the proposed coupler has a dimension of $23.245 \times 14.4\,\text{mm}^2$.

A second coupler 135°/45° that has nearly 45° between its output ports (port 3 and port 4) has been proposed, and its simulated results are depicted in Fig. 4. To realize a 45° phase difference, we made some modifications to the first coupler structure (the 90° coupler). We kept the broad bandwidth by using two-crossed transmission lines and extended the transmission line that already connects the direct and exciting ports. The purpose behind this extension is to maintain a small-sized coupler since it is well known that when the phase shift decreases, the size of the coupler may increase because the length of the transmission lines must be longer to provide the same level of coupling and isolation. Hence, a smaller phase shift requires longer transmission lines. The layout of the coupler and parameters values are given in Fig. 4. The 45° phase is achieved with the help of a Schiffman phase shifter. Herein, two identically sized Schiffman phase shifters — each measuring 7 mm — are integrated into the transmission line that links port 1 and port 3 (put symmetrically to the central vertical transmission line). This coupler has a size of $24.645 \times 13.27\,\text{mm}^2$ and covers the frequency band 4.5–8 GHz corresponding to 56% of fractional bandwidth. More importantly, the phase difference of this coupler is indicated to be −46.85° with a ±5° phase tolerance in the exciting amplitude.

3.2. Butler Matrix Configuration and Results Discussions

Based on the previously designed couplers in Subsection 3.1 a Butler matrix of a wide bandwidth has been proposed, which covers the C-band. It was simulated using the ADS software after the components were connected, and the results were further verified using a DXF file generated for the 3D electromagnetic simulator CST microwave studio. Moreover, the Butler matrix is manufactured, and its measured results are taken using a vector network analyzer (Agilent Anritsu MS2028C). For the purpose to reduce the cost, some measurements are done only for the first and second ports, since the Butler matrix has symmetry property. Fig. 5 shows the fabricated Butler matrix which is constructed on a commercially available Rogers RO4003C substrate of 3.38 relative permittivity [26]. As can be seen, with 45° phase shifters integration in the hybrid couplers and crossover removal, the proposed Butler matrix occupies a small space of $59.41 \times 55.48\,\text{mm}^2$. Remind that the input ports of the 4×4 matrix are located at its left and right extremes, and all ports are fed with a $50\,\Omega$ semiflexible coaxial line.

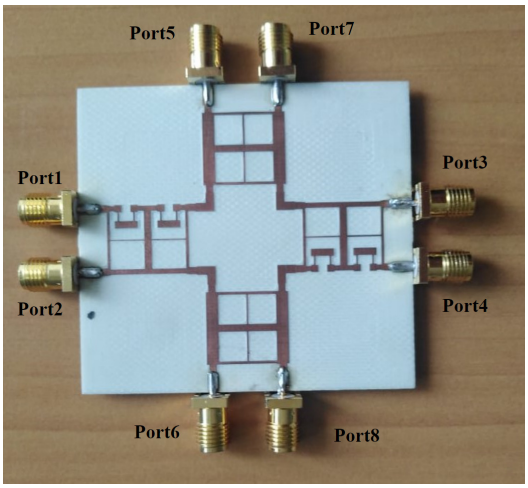

Figure 5. Fabricated prototype of the suggested Butler matrix.

Figure 6 illustrates the proposed Butler matrix S-parameter results for ports 1 and 2 as a function of frequency. As can be observed, with port 1 fed, the fractional bandwidth is 53.67% in simulation and 53.61% in measurement when the 10-dB return loss is used as the threshold. Also, the insertion loss of the Butler matrix $S(5,1)$, $S(6,1)$, $S(7,1)$, and $S(8,1)$ has a value of $-6.74(-4.92)$, $-6.38(-5.90)$, $-7.73(-7.13)$, and $-7.38(-7.96)$ dB in measurement (simulation), respectively at the frequency 6 GHz. Once port 2 gets excited, the resonance shifts a little to the right by 55 MHz, as witnessed in Fig. 6(b). The insertion loss of this port $S(5,2)$, $S(6,2)$, $S(7,2)$, and $S(8,2)$ is respectively about $-4.35(-5.83)$, $-6.61(-4.96)$, $-7.63(-7.95)$, and $-8.51(-7.09)$ dB at 6 GHz. This time the fractional bandwidth is nearly equal to 49.52%(46.15%) covering frequencies between 4.9 and 8.125 GHz in measurement, and in simulation, the band was between 5 and 8 GHz. Results from simulation and measurement show strong agreement, and the fluctuations seen in measurement can be mostly ascribed to the absence of an anechoic chamber, which helps to isolate the antenna from external radiation.

Signals produced at the input ports of the Butler matrix (from port 1 to 4) generate signals at its output ports (from port 5 to 8) with the same amplitude but have different phase discrepancies, allowing the beamforming networks to produce four beams in four different directions. It can be noticed from Fig. 7 that when port 1 is fed, the phases $\angle S(6,5)$, $\angle S(7,6)$, and $\angle S(8,7)$ are roughly $-43.6°$ at 6 GHz. The letter X in Fig. 7's legend refers to the exciting port; in other words, if the first port is fed, the phase difference between ports 5 and 6 ($\angle S(6,5)$) may be computed by subtracting the angle $\angle S(6,1)$ and angle $\angle S(5,1)$, and the other angles may be calculated in the same way. In the case that port 2 is excited, the consecutive phase difference goes to 136.96°. The phase difference of the fed ports 3 and 4 in the Butler matrix is about $-133.28°$ and 43.6°, respectively. The computed phase values have a $\pm 5°$

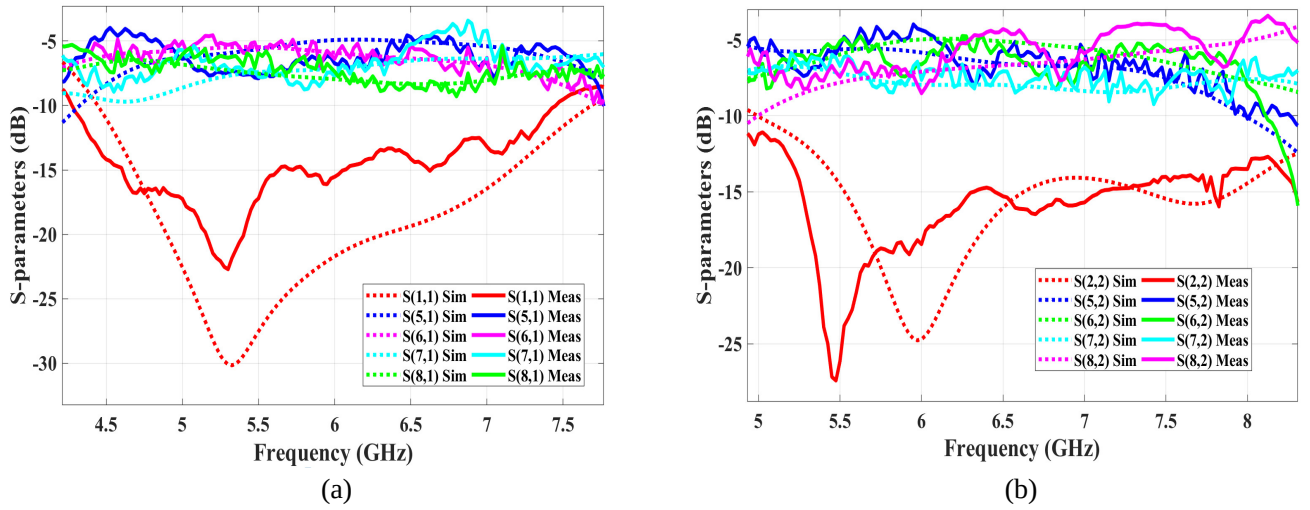

Figure 6. Suggested Butler matrix scattering parameters results, (a) port 1 fed and (b) port 2 fed.

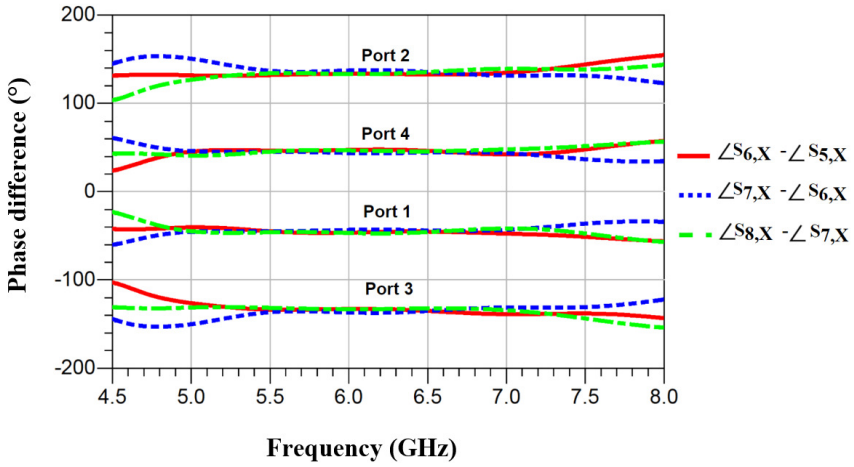

Figure 7. Phase difference of consecutive Butler matrix output ports.

phase tolerance in the entire band from 4.5 to 8 GHz. Therefore, the phase differences found at 6 GHz closely match the $\pm 45°$ and $\pm 135°$ theoretical results.

4. WIDEBAND SWITCHED BEAMFORMING ANTENNA CONFIGURATION AND RESULTS DISCUSSION

Aside from the Butler matrix, the antenna element is necessary for the implementation of beamforming networks. In this work, a four-element square-looped monopole antenna array with a partial ground plane at the button is presented and employed as the radiating element in the fabrication of the corresponding SBA array. The same Rogers substrate as in the Butler matrix is used in the construction of these antennas. We employed copper wire with a diameter of 0.6 mm, a loop with lengths and widths of 6.73 and 6.9 mm, to build the square-looped antenna element. CST microwave studio software is used to design and simulate this antenna. The reflection coefficient and realized gain obtained results are presented in Fig. 8. The suggested loop antenna's reflection coefficient graph (Fig. 8(a)) displays a good matching where its value at the center frequency of 6.21 GHz is less than -25 dB. The antenna realized gain reaches 2.68 dBi, as depicted in Fig. 8(b), which motivated us to integrate it with the suggested

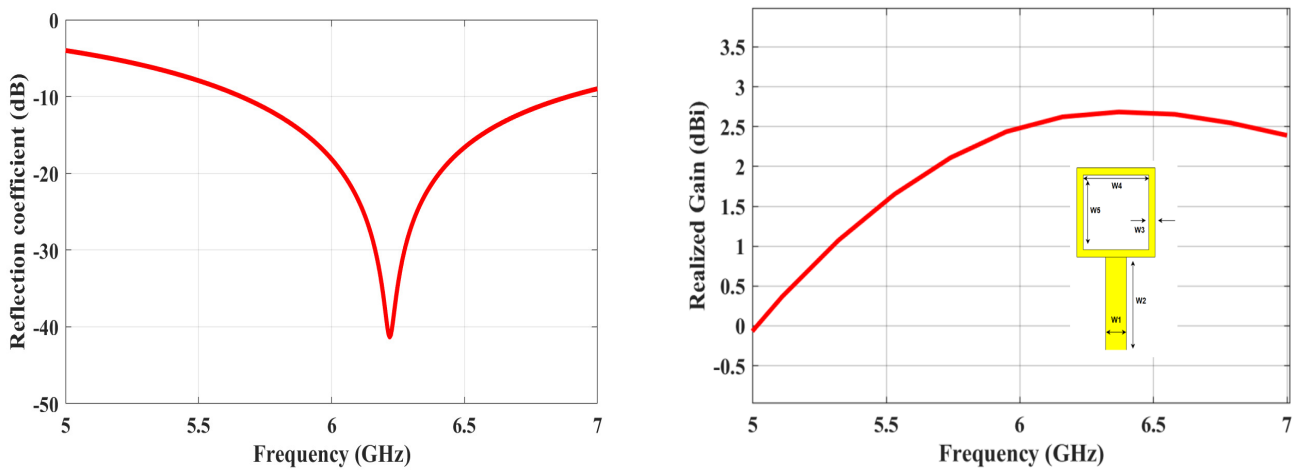

(a) (b)

Figure 8. (a) Reflection coefficient and (b) gain of the square-looped antenna element ($W1 = 2$, $W2 = 7.67$, $W3 = 0.6$, $W4 = 6.30$, $W5 = 6.13$ in mm unit).

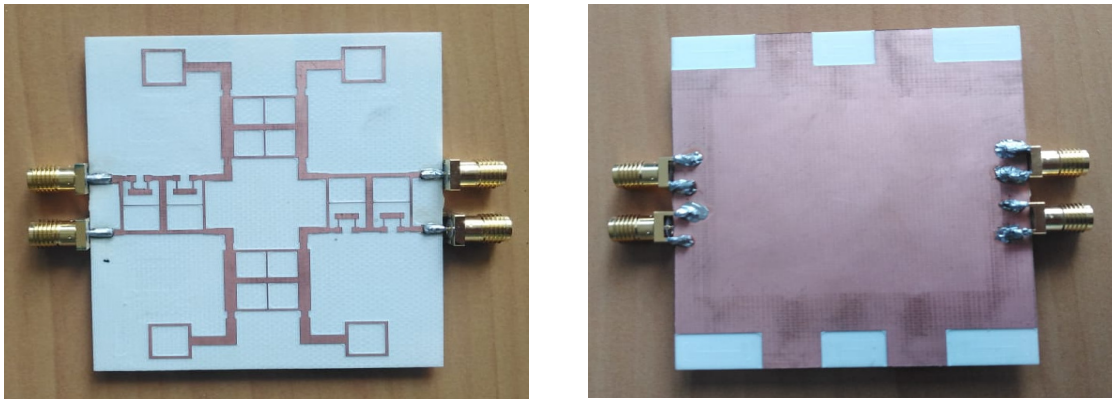

(a) (b)

Figure 9. (a) Front and (b) bottom views of the manufactured SBA array.

feeding network.

After all, the SBA system is created by attaching each antenna element to the proposed Butler matrix's output from port 5 to port 8. This antenna has been validated through a fabricated prototype shown in Fig. 9. The proposed system architecture, as demonstrated in this figure, comprises a Butler matrix with four inputs on the left and right, and four square-looped antennas fed by this Butler matrix on the top and bottom. In order to obtain a beamforming antenna with greatly reduced size, we exploited some space from the Butler matrix substrate by tilting the square-looped antennas horizontally and making the Butler matrix outputs and the feed lines of the antenna elements orthogonal. As a consequence, we were able to realize an antenna that switches its main beam toward different four directions in a single-layered substrate with a space of $70.36 \times 59.41 \times 0.81\,\text{mm}^3$ without degrading its performance. The measurement data are given in the remaining figures to demonstrate the switch beam antenna's good operation.

Figure 10 depicts the input reflection coefficients versus frequency of the suggested SBA. Herein, the results of the simulation are compared with those of the measurement. As shown in Fig. 10(a) the parameter $S(1,1)$ with a $-10\,\text{dB}$ level covers frequencies starting at 4.21 GHz and ending at 8.14 GHz, which gives a wide bandwidth of 63.64%. The switch beam antenna array has a wideband about 50.64%

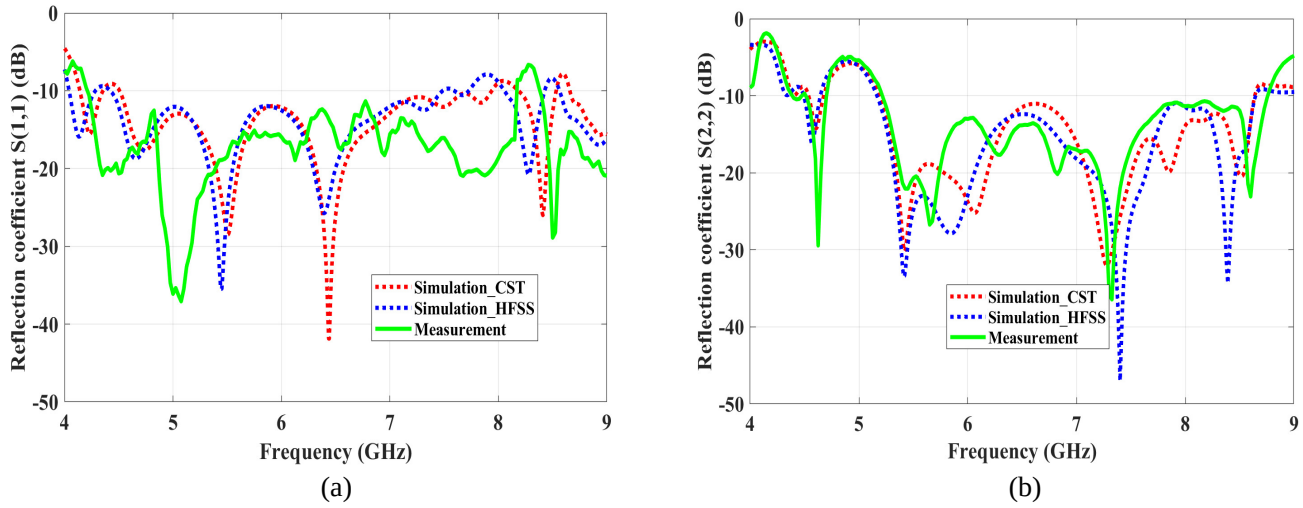

Figure 10. (a) Port 1 and (b) port 2 reflection coefficient results of the suggested SBA system.

for the parameter $S(2,2)$, corresponding to resonance between 5.22 and 8.76 GHz seen from Fig. 10(b). Although the input return loss at the second port of the beamforming antenna begins around 5.2 GHz, the antenna still has a large bandwidth. Furthermore, the plots have almost the same response when comparing the measurement with simulation, and the little difference might be ascribed to the lack of an anechoic chamber or the two different excitation mechanisms used in simulation and measurement. In measurements, a SubMiniature version A (SMA) connector has been used while in simulation the results were taken using a waveguide port. Table 1 provides the input ports' measured and simulated results.

Table 1. Proposed SBA bandwidth and working frequency in simulations and measurements.

Input Ports	Center Frequency (GHz)			Bandwidth (GHz)		
	CST	HFSS	Experiment	CST	HFSS	Experiment
Port 1	6.22	6.07	6.17	3.42	3.29	3.93
Port 2	6.91	6.9	6.99	3.43	3.46	3.54

Figures 11(a) and (b) show the radiation patterns in a polar view of the SBA at two frequencies 5.7 and 6.9 GHz, on the E-plane (Phi = 0°) when ports 1–4 are fed, respectively. As can be seen from Fig. 11(a), at 5.7 GHz, the patterns direct their main beam toward angles of −10°, 60°, −60°, and 10°, with magnitudes of 4.69, 3.95, 3.85, and 4.69 dBi for ports 1–4 excited accordingly. At 6.9 GHz (given in Fig. 11(b)), the angles at which the patterns direct the most of their radiation are −11°, 96°, −96°, and 11°, with magnitudes of 5.74, 2.72, 2.72, and 5.74 dBi, respectively. Fig. 11(c) depicts a 3D representation of the radiation pattern at 5.7 GHz as well as data comparisons utilizing CST and HFSS. Therefore, the suggested antenna was created for four-directional beamforming networks, where the main beam direction may be switched based on the exciting port. It can serve in selecting the strongest signals from among those available to ensure effective communication and avoid path loss.

Figure 12 contrasts the 5.7 GHz radiation patterns of the SBA with and without tilting the square-looped antenna elements. This figure makes it evident that the patterns are significantly better for all switched beams with good directivity, with ports 1 and 4 showing the greatest improvement. Moreover, the back lobes become negligible compared to the main beam lobes. We may thus draw the conclusion that the tilting technique generally has positive effects and enhancements on the radiation patterns, and at the same time it contributes to the reduction of the switching beam antenna dimensions.

Finally, the results of gains and radiation efficiencies of the suggested SBA over its operational

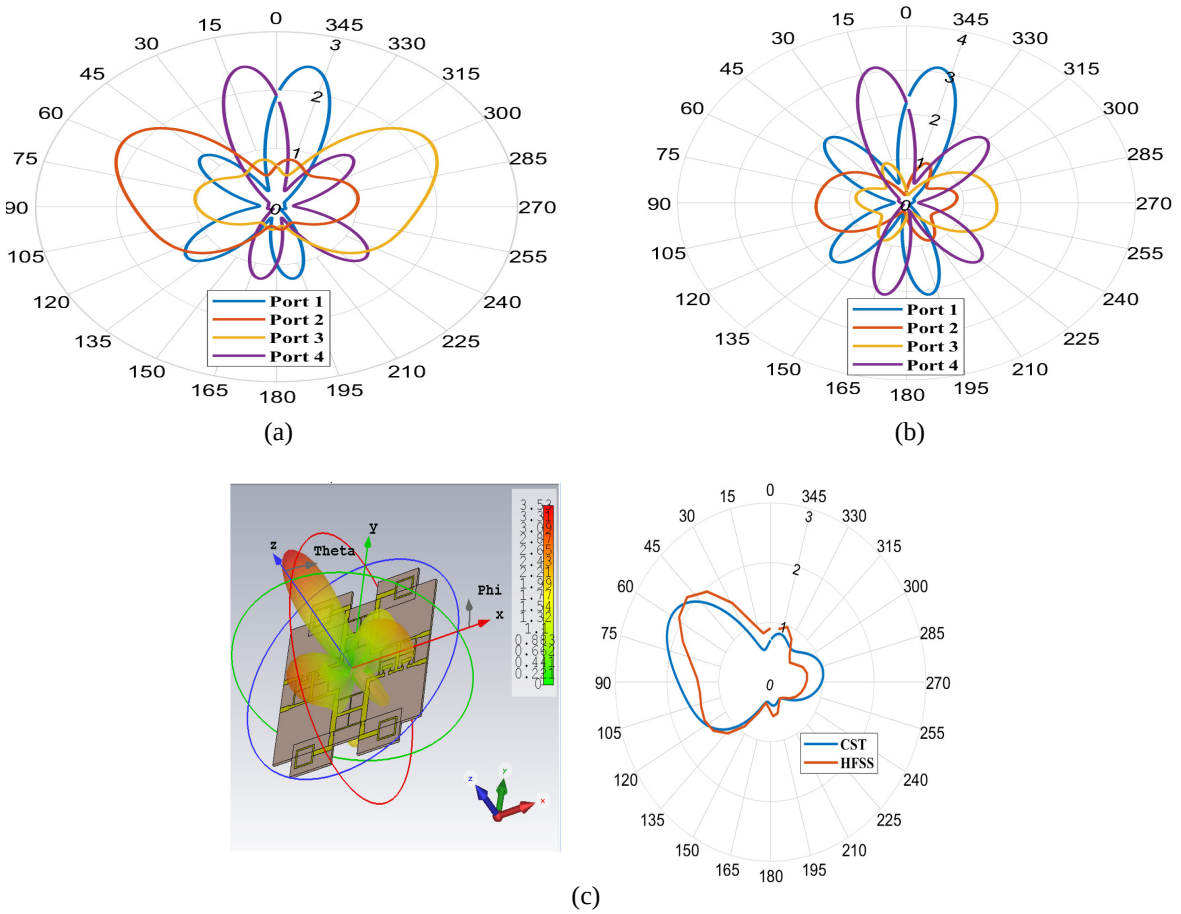

Figure 11. Radiation patterns at (a) 5.7 GHz, (b) 6.9 GHz and (c) 3D view and comparison between CST and HFSS at 5.7 GHz after exciting port 2.

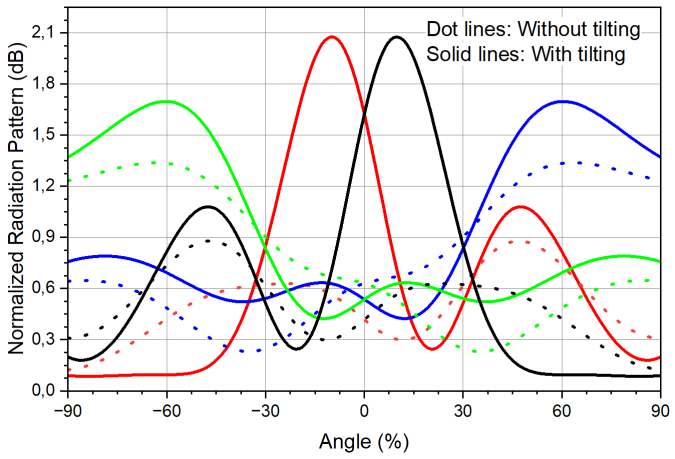

Figure 12. SBA radiation patterns with and without tilting the square-looped antenna elements at 5.7 GHz.

range are visible in Fig. 13. The left y-axis of Fig. 13(a) depicts the results of port 1 excited, whereas the right y-axis shows the results of port 2. As illustrated in this figure, the suggested antenna gain is found to be in simulation (measurement) equal to 4.24(6.80) dBi, at 6 GHz for the feeding port 1.

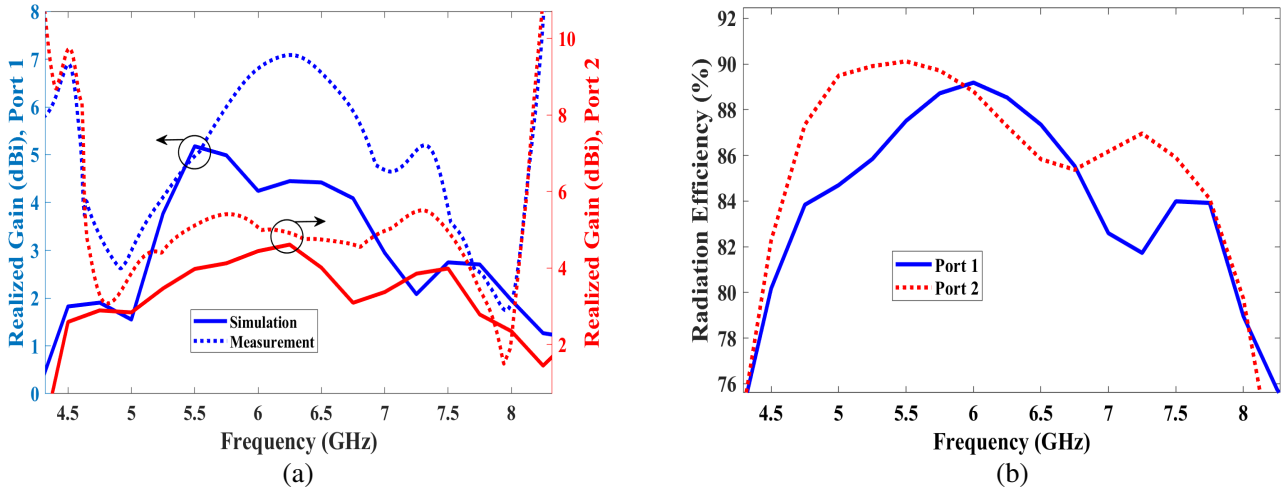

Figure 13. (a) Gain and (b) radiation efficiency results.

When port 2 is chosen as a feed, the antenna gain has a value of 4.44(5.06) dBi. It is demonstrated in Fig. 13(b) that the proposed antenna has an efficiency across the entire working band varying between 65% and 92%.

A comparison of the suggested antenna to earlier reported SBA systems which use the Butler matrix as a feeding network is provided in Table 2. In literature, a limited number of antennas — here, just [27] and [29] — operate in the same 5G frequency band as this work, while other works operate at a higher or lower frequency band. Although [28] and [30] have wider bandwidths than others (45.3% and 85.7%, respectively), they are more complicated and costly than other antennas because they use separate substrates for constructing the feeding network (Butler matrix) and the antenna. This table demonstrates how, employing a single-layer technique and the same substrate for the whole SBA system's construction, our work compromises significantly between the bandwidth of more than 63% and size reduction.

Table 2. Comparison of the proposed switched-beam antenna and similar existing antennas.

	Occupied Area (mm × mm × mm)	Beamforming Type	Beam Steering Angle (°)	Fractional Bandwidth (%)	Center Frequency (GHz)
This work	70.36 × 59.41 × 0.81	Single-Layer	±10°, ±60°	63.64	6
Ref. [27]	> 100× > 73 × 0.25	Single-Layer	±15°, ±47°	37.1	6
Ref. [28]	Butler matrix (126 × 132 × 0.81) Antenna (69 × 100 × 0.81)	Single-Layer	±42°, ±46°	45.3	2.56
Ref. [29]	Not given	Multi-Layer	±15°, ±45°	25	5.71
Ref. [24]	150.5 × 80 × 0.381	Single-Layer	±11°, ±37°	30	10
Ref. [30]	Butler matrix (128 × 117) Antenna (133 × 80)	Multi-Layer	±25°, ±70°	85.7	3.5
Ref. [31]	200 × 200 × 35.6	Multi-Layer	+9°, +26° −28°, −6°	16.15	3.75

5. CONCLUSION

This article introduces a wideband beamforming antenna array based on a simplified 4×4 Butler matrix. After this antenna was manufactured, the results from simulations and experiments were compared, and they showed good concordance. Compared to the traditional Butler matrix the crossovers were omitted, and the 45° phase shifters were integrated into the 90° hybrid couplers. It has been demonstrated that this antenna takes less space than those described in the literature, measuring $70.36 \times 59.41 \times 0.81\,\text{mm}^3$ in a single-layered substrate. It was possible to automatically change the main beam angle −10°, 60°, −60°, and 10° at 5.7 GHz by switching the antenna input ports from 1 to 4. The impedance bandwidth is approximately 63.64% and 50.64%, corresponding to the resonance bands 4.21–8.14 GHz and 5.22–8.76 GHz for ports 1 and 2 activated, respectively, with gains of 6.803 and 5.062 dBi. The efficiency of the proposed structure was up to 92%. Consequently, the suggested SBA array may be used in a variety of 5G applications since it provides a great tradeoff among manufacturing complexity, dimensions, and performance.

ACKNOWLEDGMENT

The authors of this article would like to thank Professor Angel Mediavilla of the University of Cantabria (UNICAN), Spain, for his ongoing assistance with simulations and cooperation.

REFERENCES

1. Anastasov, J., S. Panic, M. Stefanovic, and P. Spalevic, *Fading and Interference Mitigation in Wireless Communications*, CRC Press, Inc., 2017.
2. Mahender, K., T. A. Kumar, and K. S. Ramesh, "Analysis of multipath channel fading techniques in wireless communication systems," *AIP Conference Proceedings 1952*, 020050, 2018.
3. Röjsel, P., "RF MEMS-based wireless architectures and front-ends," *Handbook of Mems for Wireless and Mobile Applications*, 207–224, 2013.
4. Bembarka, A., L. Setti, A. Tribak, H. Nachouane, and H. Tizyi, "Frequency tunable filtenna using defected ground structure filter in the sub-6 GHz for cognitive radio applications," *Progress In Electromagnetics Research C*, Vol. 118, 213–229, 2022.
5. Chaipanya, P., S. Kaewuam, J. Hirunruang, W. Suntara, N. Santalunai, and S. Santalunai, "Dual band switched beam textile antenna for 5G wireless communications," *CMC — Comput. Mat. Contin.*, Vol. 73, 181–198, 2022.
6. Zulfi, J. S. and A. Munir, "Design and characterization of 4×4 Butler matrix for switched-beam antenna array," *2021 IEEE Asia Pacific Conference on Wireless and Mobile (APWiMob)*, 238–241, 2021.
7. Lialios, D. I., C. L. Zekios, and S. V. Georgakopoulos, "A compact mmWave SIW blass matrix," *IEEE International Symposium on Antennas and Propagation and North American Radio Science Meeting, APS/URSI 2021 — Proceedings*, 961–962, 2021.
8. Fakoukakis, F. and G. Kyriacou, "Novel Nolen matrix based beamforming networks for series-fed low SLL multibeam antennas," *Progress In Electromagnetics Research B*, Vol. 51, 33–64, 2013.
9. Vallappil, A. K., M. K. A. Rahim, B. A. Khawaja, N. A. Murad, and M. G. Mustapha, "Butler matrix based beamforming networks for phased array antenna systems: A comprehensive review and future directions for 5G applications," *IEEE Access*, Vol. 9, 3970–3987, 2021.
10. Zhu, J., B. Peng, and S. Li, "Cavity-backed high-gain switch beam antenna array for 6-GHz applications," *IET Microw. Antennas Propag.*, Vol. 11, No. 12, 1776–1781, 2017.
11. Rao, P. H., J. S. Sajin, and K. Kudesia, "Miniaturisation of switched beam array antenna using phase delay properties of CSRR-loaded transmission line" *IET Microw. Antennas Propag.*, Vol. 12, No. 12, 1960–1966, 2018.

12. Klionovski, K., A. Shamim, and M. S. Sharawi, "5G antenna array with wide-angle beam steering and dual linear polarizations," *2017 IEEE International Symposium on Antennas and Propagation and USNC/URSI National Radio Science Meeting*, 1469–1470, 2017.
13. Zaidel, D. N. A., S. K. A. Rahim, and N. Seman, "4×4 ultra wideband Butler matrix for switched beam array," *Wireless Pers. Commun.*, Vol. 82, No. 4, 2471–2480, 2015.
14. Tian, G., J. P. Yang, and W. Wu, "A novel compact butler matrix without phase shifter," *IEEE Microw. Wirel. Compon. Lett.*, Vol. 24, No. 5, 306–308, 2014.
15. Jeong, Y. S., and T. W. Kim, "Design and analysis of swapped port coupler and its application in a miniaturized Butler matrix," *IEEE Trans. Microw. Theory Tech.*, Vol. 58, No. 4, 764–770, 2010.
16. Bhowmik, P. and T. Moyra, "Modelling and validation of a compact planar Butler matrix by removing crossover," *Wirel. Pers. Commun.*, 5121–5132, 2017.
17. Adamidis, G., I. Vardiambasis, M. Ioannidou, and T. Kapetanakis, "Design and implementation of single-layer 4×4 and 8×8 Butler matrices for multibeam antenna arrays," *International Journal of Antennas and Propagation*, Vol. 2019, 1–12, 2019.
18. Zheng, L. M., Z. T. Lu, B. W. Xu, and S. Y. Zheng, "Flexible millimeter-wave butler matrix based on the low-loss substrate integrated suspended line patch hybrid coupler with arbitrary phase difference and coupling coefficient," *Int. J. RF Microw. Comput-Aided Eng.*, Vol. 31, No. 6, 2021.
19. Han, K., W. Li, and Y. Liu, "Flexible phase difference of 4×4 Butler matrix without phase-shifters and crossovers," *Int. J. Antennas Propag.*, 1–7, 2019.
20. Messaoudene, I., H. Youssouf, M. Bilal, and M. Belazzoug, "Performance improvement of multilayer butler matrix for uwb beamforming antenna," *Seminar on Detection Systems Architectures and Technologies (DAT)*, 1–4, 2017.
21. Jia, L., L. Zhang, and C. Zhang, "A dual-band and wide-band branch-line coupler with a large frequency ratio," *Microw. Opt. Technol. Lett.*, Vol. 63, No. 1, 146–151, 2021.
22. Bembarka, A., A. Tribak, H. Nachouane, L. Setti, and A. Mediavilla, "Wideband and electronically tunable microwave phase shifter using varactors with relative phase shifts up to 360°," *Int. J. Microw. Opt. Technol.*, Vol. 16, No. 13, 252–260, 2021.
23. Huong, H. T., "Beamforming phased array antenna toward indoor positioning applications," *Advanced Radio Frequency Antennas for Modern Communication and Medical Systems*, 2020.
24. Reddy, M. H., D. Siddle, and D. Sheela, "Design and implementation of a beam-steering antenna array using Butler matrix feed network for X-band applications," *AEU Int. J. Electron Commun.*, Vol. 147, 154147, 2022.
25. Jung, B.-R., Y.-B. Park, S.-Y. Kang, J.-H. Jung, J.-G. Ju, and Y. Yun, "Highly miniaturized on-chip 90° hybrid coupler employing transmission line with periodic structure," *PIERS Proceedings*, 1642–1644, Xi'an, China, March 22–26, 2010.
26. Substrate Rogers RO4000C series laminates data sheet, Rogers Corp., http://www.rogerscorp.com, January 6, 2023.
27. Babale, S. A., S. K. Abdul Rahim, O. A. Barro, M. Himdi, and M. Khalily, "Single layered 4×4 butler matrix without phase-shifters and crossovers," *IEEE Access*, Vol. 6, 77289–77298, 2018.
28. Wen, J. M., C. K. Wang, W. Hong, Y. M. Pan, and S. Y. Zheng, "A wideband switched-beam antenna array fed by compact single-layer butler matrix," *IEEE Trans. Antennas Propag.*, Vol. 69, No. 8, 5130–5135, 2021.
29. Nedil, M., T. A. Denidni, and L. Talbi, "Novel butler matrix using CPW multilayer technology," *IEEE Trans. Microw. Theory Tech.*, Vol. 54, No. 1, 499–507, 2006.
30. Bantavis, P. I., C. I. Kolitsidas, T. Empliouk, M. Le Roy, B. L. G. Jonsson, and G. A. Kyriacou, "A cost-effective wideband switched beam antenna system for a small cell base station," *IEEE Trans. Antennas Propag.*, Vol. 66, No. 12, 6851–6861, 2018.
31. Mousavirazi, Z., V. Rafiei, T. A. Denidni, "Beam-switching antenna array with dual-circular-polarized operation for WiMAX applications," *AEU-Int. J. Electron Commun.*, Vol. 137, 153796, 2021.